Unclassified

SECURITY CLASSIFICATION OF THIS PAGE

2

ORT DOCUMENTATION PAGE

AD-A205 589

1b. RESTRICTIVE MARKINGS

3 DISTRIBUTION/AVAILABILITY OF REPORT
Approved for public release; distribution is unlimited

2b. DECLASSIFICATION/DOWNGRADING SCHEDULE

4 PERFORMING ORGANIZATION REPORT NUMBER(S)

5 MONITORING ORGANIZATION REPORT NUMBER(S)
AFOSR-TR. 89-0307

6a NAME OF PERFORMING ORGANIZATION
University of Illinois at Chicago, CEMM Department

6b OFFICE SYMBOL (If applicable)

7a NAME OF MONITORING ORGANIZATION
AFOSR/NA

6c ADDRESS (City, State and ZIP Code)
851 S. Morgan
Chicago, IL 60607

7b ADDRESS (City, State and ZIP Code)
Building 410
Bolling AFB, DC 20332-6448

8a NAME OF FUNDING/SPONSORING ORGANIZATION
AFOSR/NA

8b OFFICE SYMBOL (If applicable)
NA

9 PROCUREMENT INSTRUMENT IDENTIFICATION NUMBER
AFOSR-88-0034

8c ADDRESS (City, State and ZIP Code)
Building 410
Bolling AFB, DC 20332-6448

10 SOURCE OF FUNDING NOS.

PROGRAM ELEMENT NO	PROJECT NO	TASK NO.	WORK UNIT NO
61102F	2302	B2	

11 TITLE (Include Security Classification) (U) Geometrical Foundations of Mesomechanics & Lagrangian Formalism

12. PERSONAL AUTHOR(S)
A. Chudnovsky, B. Kunin

13a TYPE OF REPORT	13b TIME COVERED	14 DATE OF REPORT (Yr. Mo. Day)	15. PAGE COUNT
Final	FROM _____ TO _____	January 5, 1989	35

16. SUPPLEMENTARY NOTATION

17 COSATI CODES			18 SUBJECT TERMS (Continue on reverse if necessary and identify by block number)
FIELD	GROUP	SUB GR	Mesomechanics, fractals; fracture; crack propagation

19. ABSTRACT (Continue on reverse if necessary and identify by block number)

Results of a scouting program of research in foundations of mesomechanics are presented. (a) A special case of Weyl's geometry was employed to derive equations of thermoelasticity on pure geometrical ground; this demonstrates the potential of using Weyl's geometry as a model of the geometry of the material space. (b) Experimental methods of finding fractal dimensions of fracture surfaces were examined (for various materials) together with a method of fracture profile simulation; the results contribute to developing experimental techniques of studying metric properties of the material space. (c) A new dynamic crack propagation equation was derived on the basis of the least action principle; this is a first step of applying the Lagrangian formalism to deriving equations of continuous damage evolution.

DTIC ELECTE S

20. DISTRIBUTION/AVAILABILITY OF ABSTRACT
UNCLASSIFIED/UNLIMITED ☒ SAME AS RPT ☐ DTIC USERS ☐

21 ABSTRACT SECURITY CLASSIFICATION
Unclassified

22a NAME OF RESPONSIBLE INDIVIDUAL	22b TELEPHONE NUMBER (Include Area Code)	22c. OFFICE SYMBOL
George K. Haritos	(202) 767-[redacted]	AFOSR/NA

DD FORM 1473, 83 APR EDITION OF 1 JAN 73 IS OBSOLETE.

Unclassified

SECURITY CLASSIFICATION OF THIS PAGE

~~ANNUAL~~ REPORT

to

Air Force Office of Scientific Research
(Grant No. 88-0034)

Geometrical Foundations of Mesomechanics and Lagrangian Formalism

by

A. Chudnovsky and B. Kunin
Department of Civil Engineering,
Mechanics, and Metallurgy
University of Illinois at Cicago
Chicago, IL 60680

1. Introduction

This report represents the results of the first year of a scouting program of research in foundations of mesomechanics.

Three main directions of this program outlined in the initial proposal were persued:

a) Employment of Weyl's geometry as a model of material space geometry. The potential of the approach is demonstrated in a specific example: we derive the classical equations of thermoelasticity on pure geometrical ground. This result is obtained by B. Kunin and A. Chudnovsky and is the content of Section 2.

b) Development of experimental techniques of studying metric properties of the material space. We report our first results in quantitative fractography in a search for strength parameters revealed in fracture surfaces. This work consists of two equally important parts: development of experimental technique of observation and characterization of fracture surfaces for various materials and computer simulation or erratic surface geometry. These studies are being conducted by A. Kim, B. Kunin and A. Chudnovsky and are reported in Section 3.

c) Extension of the least action principle from classical mechanics to fracture mechanics. This is the first step of application of the Lagrangian formalism to the continuous damage mechanics. At first, an introduction of a crack tip Lagrangian was thought of as a training ground for addressing the main question of continuous damage evolution. However, as the work advanced, we realized the importance of the result for understanding and description of fracture phenomena: a new dynamic crack propagation equation resulted from this approach. In the derivation of a continuous damage evolution equation, the dynamic crack propagation equation for an isolated crack will play the same role, as the Newton's equation plays in the statistical mechanics. The derivation of the dynamic crack growth equation was done by B. Gommerstadt (Northeastern University, Boston) and A. Chudnovsky and is presented in Section 4.

In Section 5 we outline future work in each of the above directions.

2. Interpretation of Thermoelasticity as a Realization of Weyl's Geometry.

The concept of damage is central to mesomechanics. In general, damage may be understood as a deviation of material morphology from its perfect (ideal) state. Thus, for example, damage in a homogeneous continuum can be visualized as distributed heterogeneity such as voids, microcracks, new phase inclusions, etc.

Usually a damage parameter is introduced as an internal variable within the framework of continuum mechanics. This approach is employed by the majority of researchers in the field of damage mechanics for the last thirty years (see a review [1] and its update [2]). Here we explore an alternative approach to modeling of damage. Following classical works in dislocation theory [3-5], we consider the internal (material) space parallel to the external (laboratory) space and the corresponding geometries. Metric properties of the internal geometry are directly related to the material morphology. Therefore, damage, as a change in the morphology, results in a change in metric properties of the material space. In our exploration of geometrical means of damage characterization, we begin with the Weyl's geometry, since this is a minimal deviation from the Euclidean geometry possessing the necessary degrees of freedom. The most lucid case of variation of a metric in the material space is thermoexpansion. Thus we reconsider

the conventional thermoelasticity as a realization of the Weyl's geometry to test the approach.

Below we define internal and external metric fields associated with a thermoelastic solid. The internal metric is intrinsic to the solid (at a given temperature), while the external metric is induced by an embedding of the solid into the laboratory space. Strain as a local measure of deviation from a stress-free state is then defined as a the difference between the two metrics. Compatibility equations for strain follow then from an apparent fact that the solid with its scaled metric associated with a non-homogeneous thermoexpansion (a special case of Weyl's Geometry) is situated in the Euclidean laboratory space. The Hook's law as a constitutive equation together with the equilibrium equations complete the system of equations. This system is shown to be equivalent to the standard equations of uncoupled thermoelastostatics.

In what follows, ξ_i will be material coordinates frozen within the solid, and χ_i will be rectilinear Cartesian coordinates in the laboratory space. It is convenient to assume that ξ_i were introduced as coinciding with the laboratory coordinates in the state of a homogeneous temperature distribution T_o and the absence of external forces (reference state). It is assumed that a thermodynamical state of an elastic solid is completely characterized by a pair $\{\underline{u}, T\}$, where $u_i = \chi_i(\xi) - \xi_i$ is

the displacement from the reference state configuration and $T = T(\underline{\xi})$ is the deviation of temperature distribution from the reference state temperature T_o. Thus the state $\{\underline{0},0\}$ is the reference state.

To remain within the scope of linear elasticity, we consider small displacement and thermoexpansion only.

The external metric g_{ij} on the solid in a state $\{\underline{u}, T\}$ describes lengths (and angles) of (and between) infinitesimal linear elements $\underline{d\xi}$ as measured in the laboratory coordinate system (so the external metric is always Euclidean). Thus it is the displacement vector $\underline{u}$ that determines $\underline{g}$. In fact,

$$g_{ij} = \sum_{k=1}^{3} X_{k,i} X_{k,j}$$

$$= \sum_{k=1}^{3} (\xi_k + u_k),i \quad (\xi_k + u_k),j$$

$$= \delta_{ij} + u_{i,j} + u_{j,i} \qquad (1)$$

neglecting the quadratic in $\underline{u}$ terms. (Here a subscript i after the comma denotes the partial derivative in ξ_i, etc.). By definition,

$$e_{ij} = \frac{1}{2}\left(u_{i,j} + u_{j,i}\right) . \tag{2}$$

Then

$$g_{ij} = \delta_{ij} + 2e_{ij} \tag{3}$$

The internal metric G_{ij} on the solid in the state $\{\underline{u}, T\}$ describes lengths (and angles) of (and between) infinitesimal linear elements $\underline{d\xi}$ as measured at a point $\underline{\xi}$ at the temperature $T_0 + T(\underline{\xi})$ in the stress-free state. The latter, for a general temperature distribution, cannot be achieved even if the external forces are turned off. The correct procedure is therefore to cut the solid into sufficiently small pieces, for each of which the conditions can be met (up to infinitesimals of higher orders). Since in the vicinity of each point the temperature distribution is homogeneous and homogeneous increase of temperature causes isotropic expansion with the factor $1+\alpha T$, then, neglecting the terms quadratic in αT,

$$G_{ij} = (1+2\alpha T)\delta_{ij} \tag{4}$$

(Kronecker's delta represents there the internal metric in the reference state due to the assumed choice of the coordinates ξ_i). The vector field $\underline{V}$ needed together with

the metric $\underset{\sim}{G}$ for defining a Weyl's geometry is equal to the gradient of the temperature field: $V_i = T_{,i}$.

The strain tensor in the state $\{\underline{u}, T\}$ is defined as

$$\varepsilon_{ij} = \frac{1}{2}\left(g_{ij} - G_{ij}\right) = e_{ij} - \alpha T \delta_{ij} \ . \tag{5}$$

From the definitions of g_{ij} and G_{ij}, it follows that stresses are related to $\underset{\sim}{\varepsilon}$ only: $\underset{\sim}{\sigma} = \underset{\sim}{\sigma}(\underset{\sim}{\varepsilon})$ and, moreover, $\underset{\sim}{\sigma}(\underset{\sim}{0}) = \underset{\sim}{0}$. Assuming The Hook's Law approximation as well, as independency of the elastic constants $\underset{\sim}{C}$ on temperature, we can write

$$\sigma_{ij} = C_{ijkl}\,\varepsilon_{kl} \tag{6}$$

The equilibrium equations are

$$\sigma_{ij,j} = f_i \tag{7}$$

where $\underline{f}$ is body force.

The missing compatibility equations appear after we compute the curvature tensor $\underset{\sim}{R}$ for $\underset{\sim}{G}$ in two ways (eqn. (11) below).

On one hand, we substitute G_{ij} by $g_{ij} - 2\varepsilon_{ij}$ (from (5)) and neglecting the terms of higher than the first order in $\underset{\sim}{\varepsilon}$ (since $\underset{\sim}{\varepsilon}$ is small), we arrive at

$$R_{kjir} = \varepsilon_{ij,kr} - \varepsilon_{ik,jr} - \varepsilon_{jr,ik} + \varepsilon_{kr,ij} \tag{8}$$

(that g_{ij} disappeared is related to the fact that g_{ij} is a Euclidean metric).

On the other hand, we substitute G_{ij} by $(1 + 2\alpha T)\delta_{ij}$ (from (4)) and neglecting the higher order terms in αT, we get

$$R_{kjir} = -\alpha(\delta_{ij}T_{,kr} - \delta_{ik}T_{,jr} - \delta_{jr}T_{,ik} + \delta_{kr}T_{,ij}) . \tag{9}$$

Comparing (9) to (8) we get the compatibility equations for strain, though written in an inconvenient form:

$$\varepsilon_{ij,kr} - \varepsilon_{ik,jr} - \varepsilon_{jr,ik} - \varepsilon_{kr,ij}$$

$$= -\alpha(\delta_{ij}T_{,kr} - \delta_{ik}T_{,jr} - \delta_{jr}T_{,ik} + \delta_{kr}T_{,ij}) . \tag{10}$$

The expressions above are antisymmetric within the pairs of indices kj and ir, therefore contracting with $\varepsilon_{lkj}\varepsilon_{mir}$ *) results in an equivalent equation with only two free indices

$$4\mathrm{Rot}_{lm}\,\underset{\sim}{\varepsilon} = 4\alpha(T_{,kk}\delta_{lm} - T_{,lm}) \tag{11}$$

or, since we assume the temperature distribution T stationary and thus $T,kk = 0$,

$$\mathrm{Rot}_{\ell m}\,\underset{\sim}{\varepsilon} = -\alpha T_{,\ell m} . \tag{12}$$

Here the operator Rot is defined by

$$\mathrm{Rot}_{\ell m}\,\underset{\sim}{p} = \varepsilon_{\ell kj}\varepsilon_{mir}p_{jr,ki} \tag{13}$$

* ε_{ijk} is the completely antisymmetric tensor with the components in Cartesian coordinates equal to +1 and -1 for even and odd permutations of 1,2,3 respectively and zero for all other combinations of indices.

for any tensor p_{ij} .

Finally, the complete system of equations is ((7), (6), (11))

$$\sigma_{ij,j} = f_i \tag{14}$$

$$\sigma_{ij} = C_{ijk\ell}\,\varepsilon_{k\ell} \tag{15}$$

$$\mathrm{Rot}_j \underset{\sim}{\varepsilon} = -\omega_{,j} \tag{16}$$

together with boundary conditions, which are assumed here to be in terms of forces. If interested in the displacement, one combines (2) and (5)

$$u_{(i,j)} = \varepsilon_{ij} + \alpha T \delta_{ij} \tag{17}$$

and solves (17) for $\underline{u}$ (upon finding $\underset{\sim}{\varepsilon}$ from (14-16).

For an isotropic material, $C_{ijk\ell} = 2\mu\delta_{ik}\delta_{j\ell} + \lambda\delta_{ij}\delta_{k\ell}$ and it is easy to see that equations (14) - (17) are equivalent to the conventional system of equations of the uncoupled quasistatic thermoelasticity. Indeed, the conventional system is (Eqs. (2.6.2) - (2.6.4) in [6])

$$\sigma_{ij,j} + f_i = 0 \tag{18}$$

$$\sigma_{ij} = \lambda \delta_{ij} e_{kk} + 2\mu e_{ij} - (3\lambda + 2\mu)\, \delta_{ij} \alpha T \tag{19}$$

$$e_{ij} = \frac{1}{2} (u_{i,j} + u_{j,i}) \tag{20}$$

Here the displacement field $\underline{u}$ is considered a primary variable ($\underset{\sim}{\varepsilon}$ is a derived variable). Then $\underset{\sim}{e}$ identically satisfies (16) (with (2), (5) taken into account). In the preceeding exposition, the strain $\underset{\sim}{\varepsilon}$ is the primary variable and the displacement can be reconstructed using (17).

The geometry utilized above is a very special case of Weyl's geometry. General Weyl's geometry is more rich and appears adequate for modelling distributed damage.

References

[1] D. Krajcinovic, Continuum Damage Mechanics, Applied Mechanics Reviews, Vol. 37:1-6 (1984), 397-402.

[2] D. Krajcinovic, Update to "Continuum Damage Mechanics," Applied Mechanics Update, 1986.

[3] K. Kondo, Memoirs of the Unifying Study of the Basic Problems in Engineering Sciences by Means of Geometry, v.1, Tokyo, Gakujutsu Bunken Fukyu-Kai.

[4] B. A. Bilby, R. Bullough, E. Smith, Continuous Distributions of Dislocations: A New Application of the Methods of Non-Riemannian Geometry, Proc. Roy. Soc. London, Ser. A, 231, 263-273.

[5] I. A. Kunin, A supplement to J. A. Schouten's "Tensor Analysis for Physicists," Moscow, 1965 (in Russian); available in English from the U. S. Dept. of Commerce, Springfield, VA 22151.

[6] B. A. Boley and J. H. Weiner, "Theory of Thermal Stresses," John Wiley & Sons, N. Y., 1962 (2nd ed.)

3. Fracture Surface Characterization

It is generally understood that material toughness and specific fracture energy are higher for more erratic fracture surfaces. Fractal geometry suggests parameters to quantify erraticism of crack surfaces. One of them is the crack diffusion coefficient used in the 'crack diffusion model' of brittle fracture [1]. Other characteristics are supplied by fractal studies: fractal dimension D of a fracture surface (profile) together with basic patterns ("generators") on various scales.

To study the correlation between D and material toughness, one needs

a) to determine which of the existing techniques of experimental evaluation of D is most suitable for a given material,

b) to analyze the consistency of an experimental procedure under consideration.

3.1 Some Methods of Finding Fractal Dimension

There are two approaches to finding the fractal dimension (D) of a fracture surface: Profile Analysis and Surface Analysis. Figures 1 and 2 represent the two approaches schematically.

3.2 Outline of Performed Studies

Profile Analysis

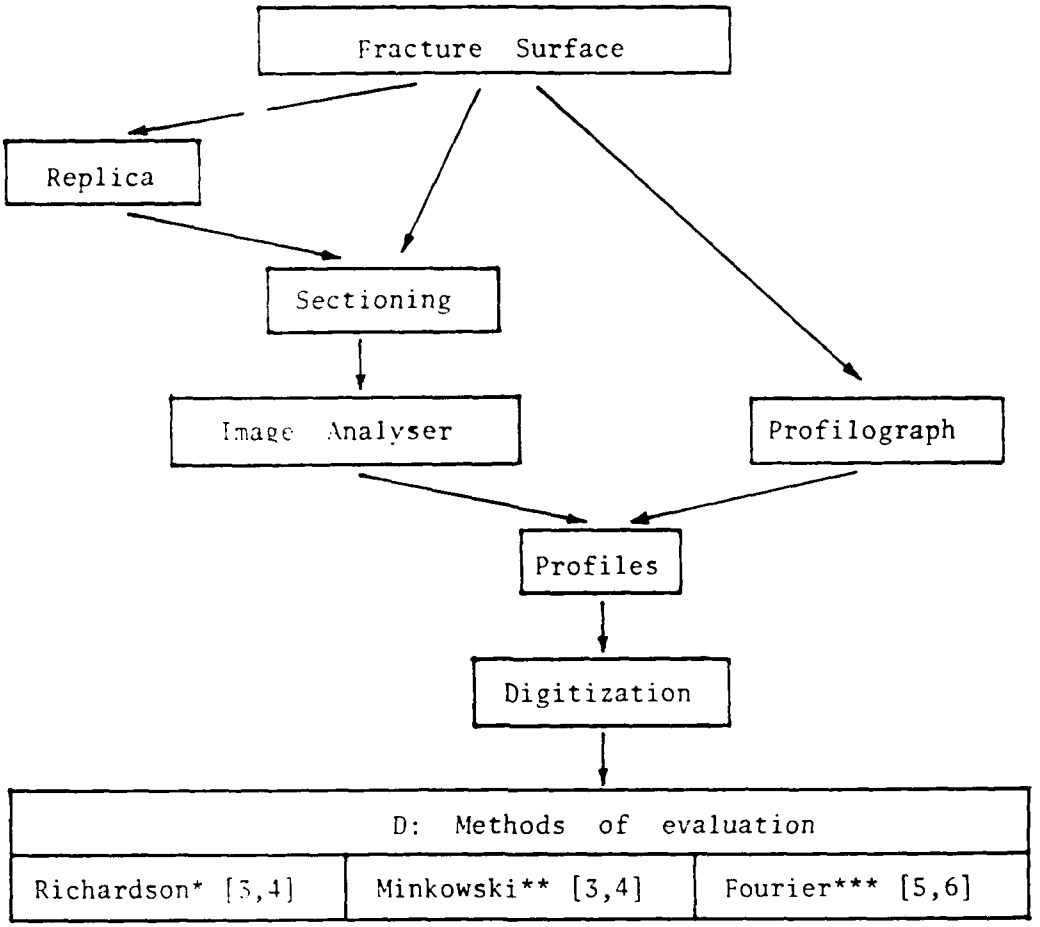

* Richardson's method uses a sequence of measurements of the "length" of a profile utilizing a compass of decreasing opening, i.e. a sequence of lengths of increasingly fine polygonal approximations of the profile. Also known as the "measuring stick technique".

** Minkowski's method of determining D of a planar profile utilizes a sequence of areas of thinner and thinner strips, each obtained as a result of uniform thickening of the profile. The ratios of the areas to the strip widths are analogs of polygons in the Richardson's method.

*** The Fourier Transform method utilizes the sequence of Fourier coefficients of the profile, specifically, the rate of their convergence to zero. The lengths of the graphs of harmonics in the profile's Fourier series are analogs of the lengths of polygons in the Richardson's method.

Figure 1

Surface Analysis

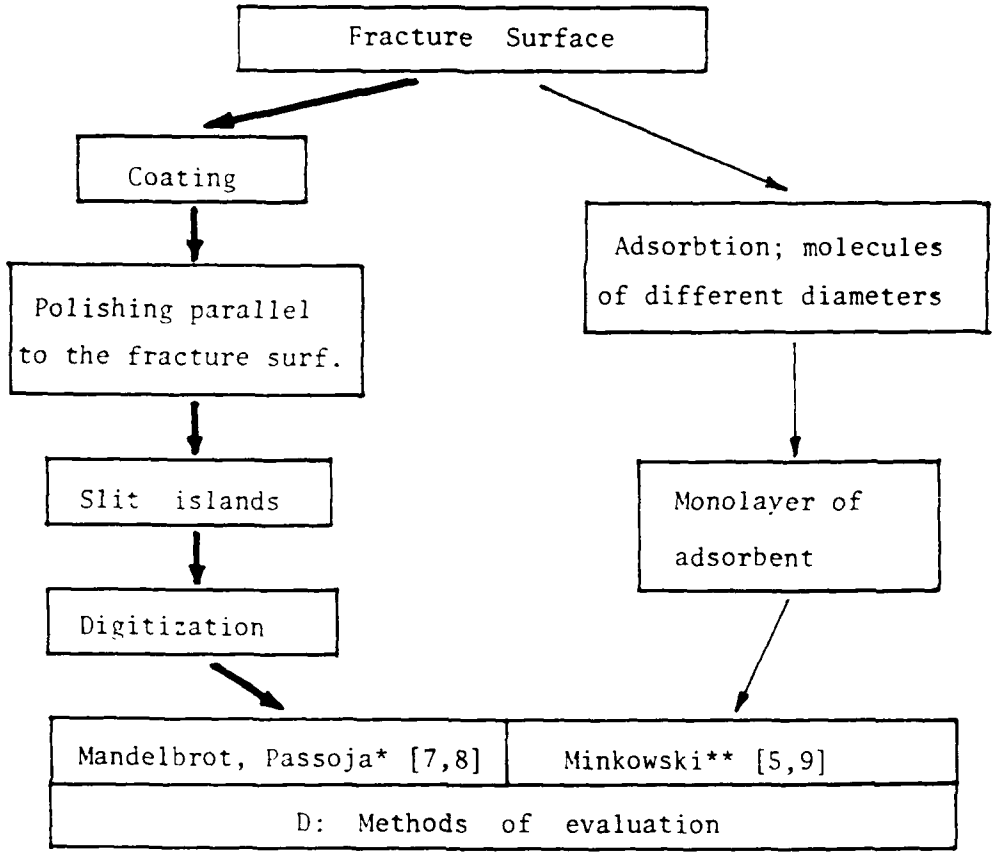

* "Slit island analysis" of Mandelbrot and Passoja (thick arrows above) utilizes a D-dependent relation between areas and perimeters of slit islands, as the latter appear and grow in the plane of polish.

** Minkowski's method of determining D of a surface in 3-space uses a sequence of thinner and thinner layers, each obtained as a result of a uniform thickening of the surface. (The ratio of the volume of the layer to its thickness is an approximation to the surface's "area".)

Figure 2

The experimental program conducted in the first year consisted of a few steps.

a) Analysis of which of the existing experimental techniques is most suitable for a particular material (see Figs. 1, 2). Our model materials were: graphite (which exhibits typical features of fracture surfaces associated with brittle failure of polycrystalline materials) and polyethylene (with highly fibrillated fracture surfaces typical for many engineering plastics).

b) Application of particular techniques to the model materials. The "slit island" method was applied to graphite and the Richardson's plot method to both graphite and polyethylene.

c) Computer simulation of fractal trajectories by means of Fourier synthesis. Comparison of the simulated trajectories with the observed profiles.

In Figs. 1,2 we summarized most popular techniques of fractal dimension evaluation. There are two techniques applied directly to surfaces. The absorption method leaves, in our opinion, an uncertainty due to the limitations in controlling the uniformity of coating thickness. The "slit island" method appears straightforward and has been employed. It remains to be seen how sensitive it is to the orientation of the plane of polish.

Out of the three methods applicable to fracture profiles, the Fourier technique seems more promising, but it requires software that we do not have at present. The other two methods are similar in their limitations and advantages; we employed the Richardson's plot method.

Below we report our results in application of the "slit island" and Richardson's plot techniques.

3.3 "Slit Island" Technique

The fracture surface was obtained from a compact tension graphite specimen. Figure 3 shows a general view of

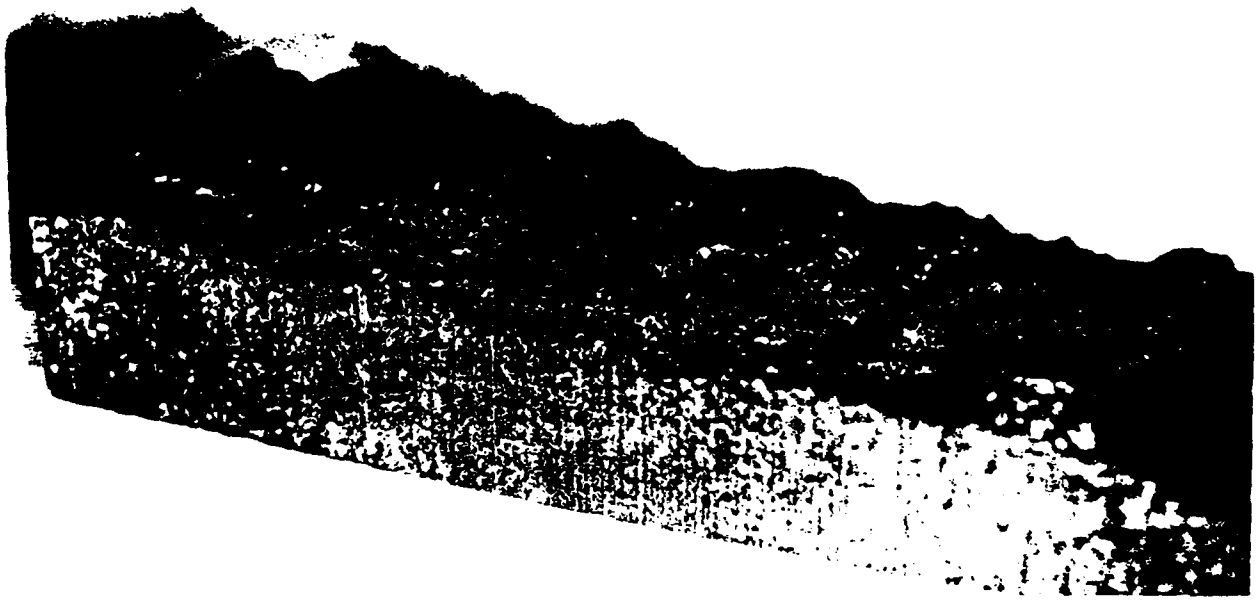

Fig. 3

the fracture surface. To proceed with comparative studies of different techniques, multiple wax replicas of the fracture surface were made and "shaving" was performed on

The replica. A typical replica is shown in Fig. 4. The light and dark areas represent the two faces of the crack.

Fig. .

Fig. . The essence of the technique together with a "artificial" replica.

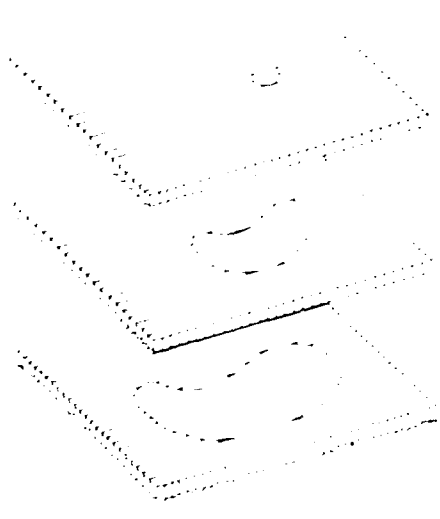

Figure 6 shows the Image Analyzer screen with an island. The image can be digitized and its area and perimeter (required by the procedure) are evaluated automatically.

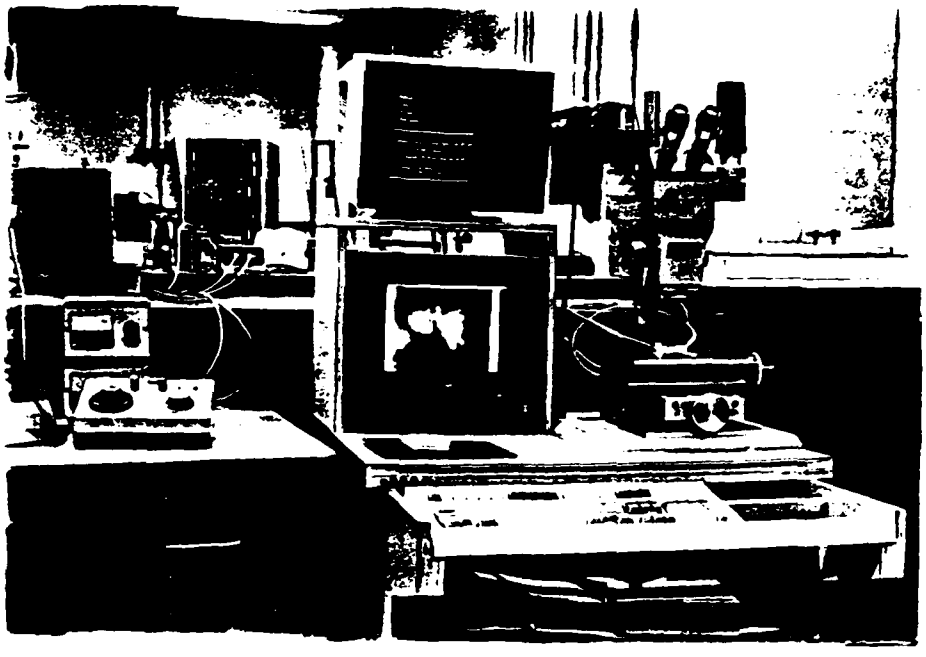

Fig. 6

Figure 7 shows the observed area vs. perimeter relationship (dots) and its approximation by a straight line.

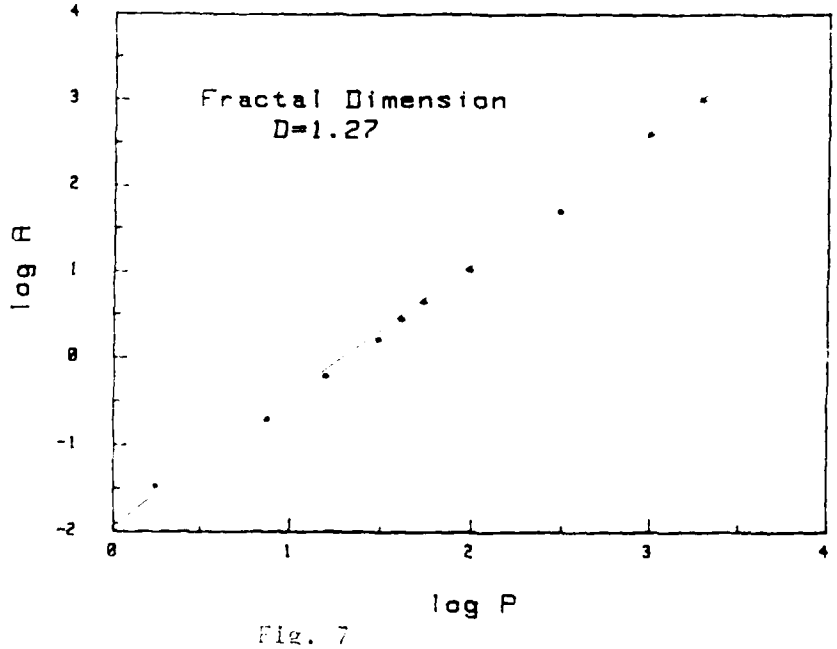

Fig. 7

The line's slope $k = 1.57$ yields the fractal dimension of the fracture surface: $D = 1 + 2/k = 2.27$.

3.4 Richardson's Plot Technique

For graphite, the fracture profiles were obtained from the specimen shown in Fig. 3 above. Wax replicas were used again to preserve the specimen. A typical profile is shown in Fig. 8.

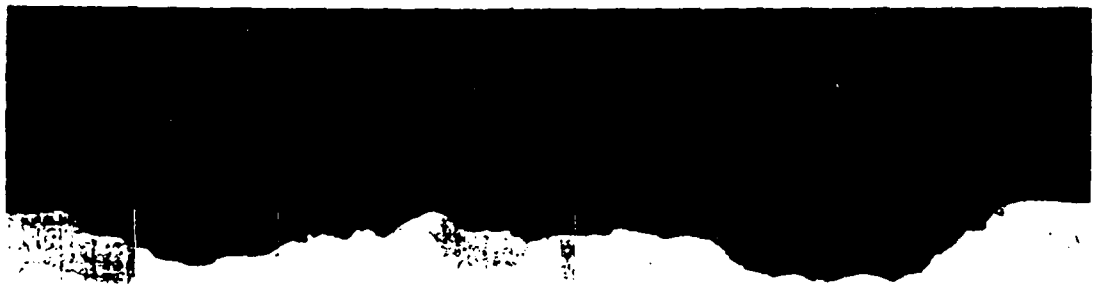

Fig. 8

Figure 9 shows the observed profile's "length" L as a function of the compass opening (dots) together with the straight line approximation of the relation.

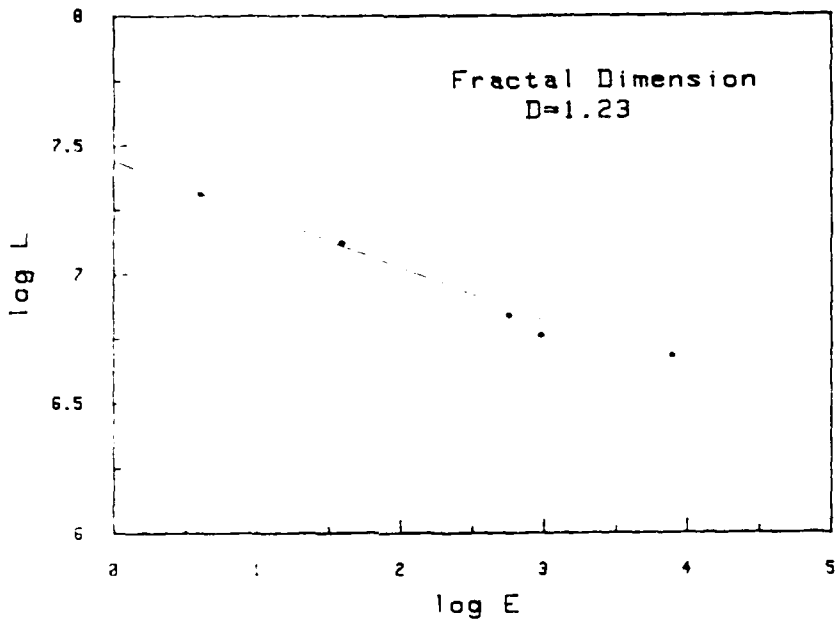

Fig. 9

The slope $k = -0.23$ of the straight line yields the fractal dimension of the profile: $D = 1 - k = 1.23$, i.e. the dimension $1+D = 2.23$ of the fracture surface.

Fig. 10

For a fatigue fracture surface in polyethylene (Fig. 10), figures 11,12 show a typical fracture profile (parallel to the crack front) and the profile-length-vs.-compass-opening relationsnip.

Fig. 11

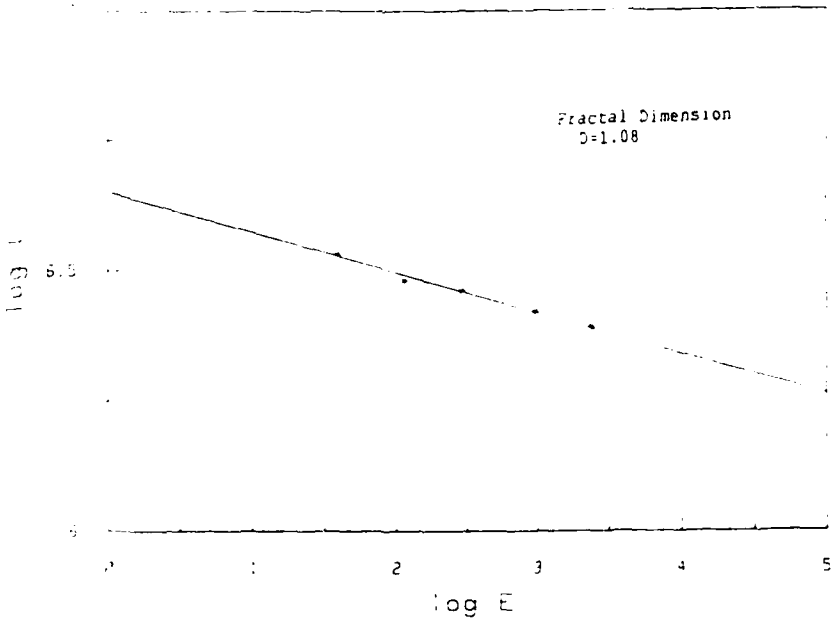

Fig. 12

The slope $k = -0.08$ of the straight line in Fig. 12 yields $D = 1.08$ for the profile.

3.5 Profile Simulation

To simulate the profile from Fig. 8 the following relation between the fractal dimension of a curve and the rate of decrease of the curve's Fourier coefficients [5]. If a function $f(x)$ is expanded in a Fourier series

$$f(x) = a_0 + \sum_{k=1}^{\infty} a_k \sin(kx + \rho_k)$$

and $a_k \sim k^{-\alpha}$ as $k \to \infty$, then the graph of the function $f(x)$ has (generically) the fractal dimension $D = 2-\alpha$.

We generated sequences of coefficients a_k by calling a random number generator (for each k), which supplied us with a random number r_k equidistributed between 0 and 1, and then put $a_k = (2r_k - 1)k^{-\alpha}$, so that a_k is equidistributed between $(-k^{-\alpha})$ and $k^{-\alpha}$.

Figure 13 shows a curve obtained for $D = 1.23$ ($\alpha = 2-D = .77$). The Fourier series was truncated to 500 terms; a_0 and all ρ_k were put equal to zero for simplicity.

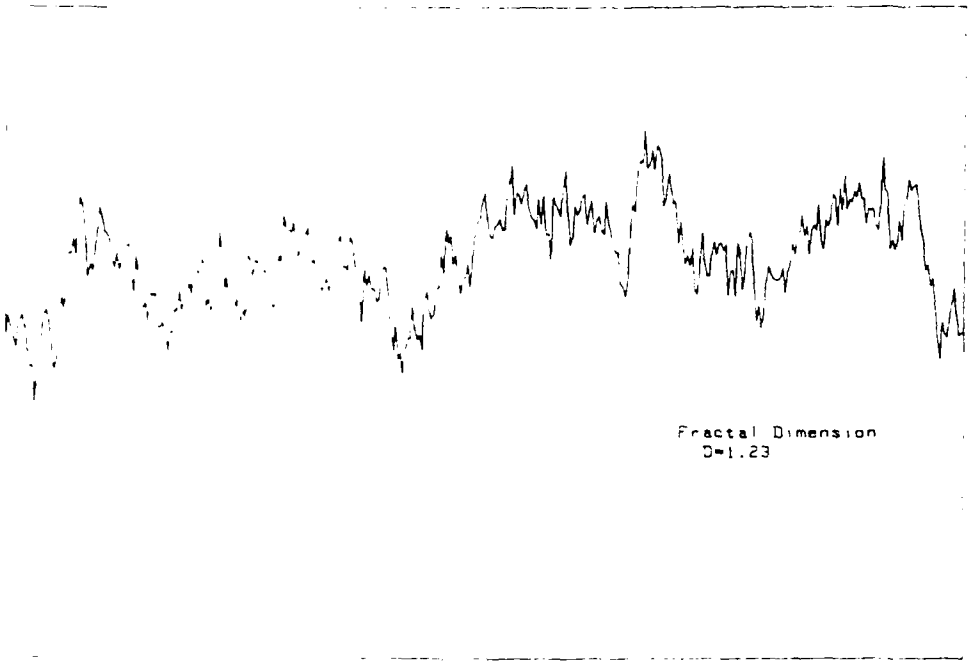

Fig. 13

3.6 Conclusions

Extensive experimentation leads us to the following conclusions.

1. We possess adequate techniques of evaluation of fractal dimension.

2. Fractal dimension alone is insufficient for adequate simulation of fracture profiles (Fig. 13 clearly does not mimic the original profile). One needs additional characteristics: basic patterns ("generators"), scale dependency, etc.

References

[1] A Chudnovsky and B. Kunin, A probabilistic Model of Brittle Crack Formation, J. Appl. Phys., 62 (10), 4124-4129 (1987).

[2] J. J. Mecholsky, D. E. Passoja and K. C. Feinberg, "Quantitative Analysis of Brittle Fracture Surfaces Using Fractal Geometry," submitted to J. Am. Cer. Soc. (1986).

[3] M. Coster, J. Chermant, "Recent Developments in Quantitative Fractography," International Metals Reviews, vol. 28, No. 4 (1983), 228-250.

[4] B. Mandelbrot, "Fractal Geometry of Nature," Freeman, San Francisco, 1982.

[5] P. Pfeifer, Fractal Dimension as Working Tool for Surface Roughness Problems, J. Appl. Surf. Sci. (1984).

[6] D. E. Passoja and D. J. Amborski, "Fracture Profile Analysis by Fourier Transform Methods," Microstructural Science, 6, 143-148 (1978).

[7] B. Mandelbrot, D. Passoja, A. Paullay, "Fractal Character of Fracture Surfaces of Metals, Nature, vol. 308 (1984), 721-722.

[8] B. B. Mandelbrot, D. E. Passoja and A. J. Paullay, "Fractal Character of Fracture Surfaces of Metals," Extended Abstracts in Fractal Aspects of Materials: Metal and Catalyst Surfaces, Powders and Aggregates, eds. B. B. Mandelbrot and D. E. Passoja, MRS, Pittsburgh, PA, pp. 7-9 (1984).

[9] P. Pfeifer, D. Avnir, "Chemistry in Noninteger Dimensions Between Two and Three..." J. Chem. Phys., 79 (7) (1983), 3558-3565.

4. Dynamic Crack Growth Equation

4.1 Introduction

The kinetics of fast crack propagation has been discussed since the pioneering work by Mott[1] for the last 40 years.

A choice of a fundamental assumption which leads to dynamic crack propagation equation is the key point of the discussions. Proposed by Eshelby[2,3] and presently widely accepted way to derive dynamic crack growth equation "is to suppose, along with A. A. Griffith, that the energy released at the top is all used to provide the surface energy (γ) of the faces of the crack. This gives the equation of motion" (quoted from ref. 2):

$$G_1^d(\ell, \dot{\ell}) = 2\gamma \quad , \tag{1}$$

where G_1^d is the dynamic energy release rate with respect to the crack tip advance and ℓ and $\dot{\ell}$ are the crack length and velocity respectively. (2-D problem is considered). Achievements, limitations and difficulties of dynamic crack growth theories as well as the comparison with experimental data are quite adequately presented in several reviews, for instance Erdogan[4] and Rose[5].

Here we empnasize one problem which is associated with the nature of dynamic crack extension. It follows from elastodynamic solution, that the dynamic energy release rate does not depend on crack tip acceleration. Thus, if the crack tip is regarded as a particle, then it is the one which exhibits no inertia. It is a puzzling result. Indeed, a crack can be formally represented as a continuous array of dislocations moving, when the crack extends. It is also well known that every individual dislocation possess an "inertia".

However a pile of them loses this feature. Eshelby[6] suggested a possible explanation: "In a limit of a large number of dislocations, their mutual interactions entirely dominate their individual properties". This guess still remains unconfirmed. Beside this theoretical difficulties, there are experimental evidences, that a dynamic crack exhibit inertial behavior[7,8]. One of such observations stimulated present study. We consider an alternative approach to the derivation of dynamic crack growth equation: we define a crack tip Lagrangian employing elastodynamic solution and then apply the Least Action principle to select the actual crack tip motion from an ensemble of all possible ones.

4.2 Kinetics of Crack Propagation

We limit our consideration to a rectilinear crack propagating through a homogeneous, isotropic, linear elastic solid.

Let us consider, the conventional Lagrangian density of elastodynamics:

$$\mathcal{L} = k - f \,, \tag{1}$$

where $k = \frac{1}{2}\,\rho(x_\alpha)\dot{u}_i\dot{u}_i$ - stands for kinetic energy density $f = \frac{1}{2}\,u_{i,j}\,C_{ijk\ell}\,u_{k,\ell}$ is the strain energy density, ρ and $\underset{\sim}{C}$ are the density and the elastic moduli tensor, x_i is Cartesian coordinate, x_o, u_i, $u_{i,j}$ and $\dot{u}_i$ are the time, displacement vector, displacement gradient, and the velocity components respectively. Latin and Greek subscripts take values $i,j,k, = 1,2,3$ and $\alpha,\beta = 0,1,2,3$.

The global Lagrangian of an elastic solid V can be obtained by integrating over the volume V:

$$L = \int_V \mathcal{L}\,dv \,. \tag{2}$$

Then conventional action results from the integration of L with respect to time.

Variation of the action with respect to displacement leads to conventional equations of elastodynamics $\rho\ddot{u}_i = \partial_j \left(\frac{\partial f}{\partial u_{i,j}}\right)$. The following balance equations also hold:

$$\left(\frac{\partial \mathcal{L}}{\partial x_\alpha}\right)_{exp} = -\frac{\partial P_{\alpha\beta}}{\partial x_\beta} \tag{3}$$

Here $\left(\partial/\partial x_\alpha\right)_{exp}$ means the derivation with respect to x_α when the rest variables are held fixed and $P_{\alpha\beta}$ is the 4X4 elastodynamic energy momentum tensor, introduced by Eshelby[3,6]:

$$P_{\alpha\beta} = -\mathcal{L}\,\delta_{\alpha\beta} + \frac{\partial \mathcal{L}}{\partial u_{\alpha,\beta}}\, u_{\delta,\alpha}$$

The components of energy momentum tensor can be expressed in terms of kinetic and strain energy densities, stress, strain and displacement:

$$\begin{aligned} P_{ij} &= (f - k)\,\delta_{ij} - \sigma_{k,j}\, u_{k,i} \\ P_{ko} &= u_i\, u_{i,k} \\ P_{oj} &= -\sigma_{ij}\, u_i \\ P_{oo} &= f + k \end{aligned} \tag{4}$$

We consider a crack in a plane x_1, x_3 with a straight front along parallel to x_3 moving in x_1 direction. Then the crack front location is determined by x_1-coordinate $x_1 = \ell(x_o)$, where ℓ is the crack length, x_o stands for time. We describe the crack as a singularity (zero-values in density and elastic moduli along the crack) Thus,

$$\rho(x_\alpha) = \rho(x_1 - \ell) \quad , \tag{5}$$

$$\underset{\sim}{C}(x_\alpha) = \underset{\sim}{C}(x_1 - \ell) \quad ,$$

and consequently

$$\frac{\partial \mathcal{L}}{\partial x_1}_{exp} = - \frac{\partial \mathcal{L}}{\partial \ell} \tag{6}$$

From eqs (2), (3) and (6) we arrive at

$$\frac{\partial L}{\partial \ell} = \int_V \frac{\partial P_{1\beta}}{\partial x_\beta} dv \tag{7}$$

Applying it we introduce a crack Lagrangian $L^c(\ell, \dot{\ell})$:

$$L^c(\ell, \dot{\ell}) = \int_0^\ell \frac{\partial \mathcal{L}^c}{\partial \ell} d\ell + L_0^c(\dot{\ell}) \tag{8}$$

where

$$\frac{\partial \mathcal{L}^c}{\partial \ell} = \lim_{V \to 0} \int_V \partial_\beta P_{1\beta} dv \quad \text{and} \tag{9}$$

$\mathcal{L}_0^c(1)$ can be evaluated as $\mathcal{L}^c(\ell, \dot{\ell})$ at $\ell \to 0$

The definition (9) is based on the assumption that the elastic field within an infinitesinal vicinity of the crack tip only governs crack propagation. Apparently, L^c is only a part of the total Lagrangian of a solid with the crack. Now we apply the Lagrangian technique to formulate the dynamic crack motion equation as an Euler-Lagrange eq. associated with L^c:

$$\frac{d}{dX_0} \frac{\partial L^c}{\partial \dot{\ell}} - \frac{\partial L^c}{\partial \ell} = -2\gamma, \tag{10}$$

where the specific energy of new surface formation 2γ appears as the energy sink.

To specify eq. (10) we need to account for the elastic field near the crack front. In this region the asymptotic displacement field can be expressed as $u(X_1, X_2, X_0) = u(X_1 - x_0, X_2)$ and consequently

$$\partial_0 = -\partial_1 = \partial ,$$

It can be shown (see for instance [5]) that the integrand of eq. (9) can be presented in the divergence form:

$$\partial_\beta P_{1\beta} - \frac{\partial P_{1j}}{\partial X} + \frac{\partial P_{10}}{\partial X_0} = \partial_j H_{1j} \qquad (11)$$

where $H_{ij} = (\varepsilon \cdot k)\,\delta_{ij} - \sigma_{kj} u_{k,i}$. Then following the conventional notations we introduce a dynamic energy release rate[5].

$$G_1^d(\ell, \dot{\ell}) = \lim_{v \to 0} \int_{\partial V} H_{ij}\, n_j \, d \quad , \qquad (12)$$

where n_j is the unit outer normal to the boundary ∂V

As has been shown[3] G_1 can be factorized:

$$G_1^d(\ell, \dot{\ell}) = g(\dot{\ell})\; G_1(\ell) \qquad (13)$$

where $G(\ell)$ is the conventional static energy release rate per unit crack advance, $g(\dot{\ell})$ is the velocity factor.

Upon substitution (13) into (8) we obtain:

$$L^c(\ell, \dot{\ell}) = g(\dot{\ell})\; \Pi(\ell) \quad , \qquad (14)$$

where $\Pi(\ell)$ is the potential energy of the solid associated with the crack. The term L_o^c on (8) vanishes since $L^c(\ell, \dot{\ell})$ tends to zero with $\ell \to 0$. The latter follows from Kostrov's solution for dynamic stress intensity factor for a crack suddenly appearing in an initially continuous solid.[9]

Making use of (14) and (10) we arrive at the following crack propagation equation

$$m(\ell,\dot{\ell})\ddot{\ell} = F(\ell,\dot{\ell}) \quad , \tag{15}$$

here we designate 'm' as a crack inertia coefficient (CIC)

$$m(\ell,\dot{\ell}) = \Phi(\dot{\ell})\ \Pi(\ell) \quad , \tag{16}$$

and the crack driving force

$$F(\ell,\dot{\ell}) = \Phi(\dot{\ell})\ G_I(\ell) - 2\gamma(\dot{\ell}) \tag{17}$$

$$\Phi(\dot{\ell}) = \frac{1}{c^2}\ \frac{d^2 g(M)}{dM^2}$$

$$\Psi(\dot{\ell}) = g(M) - M\ \frac{dg(M)}{dm}$$

$$M = \dot{\ell}/C$$

4.3 Discussion and Conclusions

Since, m and F do not depend on $\ddot{\ell}$, then, according to eq. (15) a crack propagation appears as a pseudoparticle motion with a "mass" being proportional to the potential energy associated with a crack. The crack driving force represents the excess of energy release rate above the required fracture energy 2γ.

The expression $G_I(\ell)$ for various loading conditions and specimen configurations is readily available [10]. The velocity factors $g(\dot{\ell})$ and consequently $\Psi(\dot{\ell})$ and $\Phi(\dot{\ell})$ require a solution of elastodynamic problem and have an exact solution for only a few specific loading conditions.

An illustrative example of the dynamic anti-plane crack growth equation is presently in preparation.

We have two concluding remarks to make.

1. The crack propagation equation needs an experimental examination.
2. It is well known that fracture surfaces created at different crack speeds exhibit different roughness. In a continuum based model outlined in this section, the roughness of a fracture surface can be accounted for by a dependency of the specific fracture energy on the crack speed: $\gamma = \gamma(\dot{\ell})$.

REFERENCES

1. N. F. Mott, Engineering, Lond. 165, 16(1948).

2. J. D. Eshelby, J. Mech. Phys. of Solids, 17, 177 (1969).

3. J. D. Eshelby, Sci. Prog., Oxf. 59, 161 (1971).

4. F. Erdogan, 'Crack Propagation Theories', Fracture, Vol. II, H. Liebowitz (ed.), Academic, N. Y., 497 (1968).

5. L. R. F. Rose, Int. J. Fracture, 12, 799 (1976).

6. J. D. Eshelby, in Prog. Solid State Physics, F. Seitz and D. Turnbull (ed.), Vol. 3, 79 Academic, N. Y. (1956).

7. J. Botsis, A. Chudnovsky, J. Fracture, 33,R67 (1987).

8. D. E. Grady J. appl. Phys. 53(1) (1982).

9. B. V. Kostrov, J. Appl. Math., Mech, 28, 793 (1964).

10. Stress Intensity Factors Handbook Editor-in-chief Y. Murakami, Pergamon Press, 1987.

5. Future Work

We consider the following tasks as a logical continuation of the research outlined above.

a) To formulate the kinematics of a continuum theory of defects (state variables, compatibility) on the basis of the Weyl's geometry.

b) To develop a methodology of experimental evaluation of the parameters of the Weyl's geometry (fractal type characteristics at various scales).

c) To expand the Lagrangian formalism to media with evolving damage; to combine the resulting constitutive laws with the obtained compatibility equations and the equilibrium equations and examine the entire model experimentally.

d) To develop and examine experimentally a model for defect nucleation to account for processes occurring in the material before the Lagrangian formalism takes over.